AFRL-RQ-WP-TM-2013-0142

COMPUTATIONAL ANALYSIS OF DIFFUSER PERFORMANCE FOR THE SUBSONIC AERODYNAMIC RESEARCH LABORATORY (SARL)

Tom A. Presdorf

Aero Validation Branch
Aerospace Vehicles Division

Christopher D. King, Semih M. Ölçmen, and Muhammad A.R. Sharif

The University of Alabama

FEBRUARY 2013
Interim Report

Approved for public release; distribution unlimited.

See additional restrictions described on inside pages

STINFO COPY

AIR FORCE RESEARCH LABORATORY
AEROSPACE SYSTEMS DIRECTORATE
WRIGHT-PATTERSON AIR FORCE BASE, OH 45433-7542
AIR FORCE MATERIEL COMMAND
UNITED STATES AIR FORCE

NOTICE AND SIGNATURE PAGE

Using Government drawings, specifications, or other data included in this document for any purpose other than Government procurement does not in any way obligate the U.S. Government. The fact that the Government formulated or supplied the drawings, specifications, or other data does not license the holder or any other person or corporation; or convey any rights or permission to manufacture, use, or sell any patented invention that may relate to them.

This report was cleared for public release by the USAF 88th Air Base Wing (88 ABW) Public Affairs Office (PAO) and is available to the general public, including foreign nationals.

Copies may be obtained from the Defense Technical Information Center (DTIC) (http://www.dtic.mil).

AFRL-RQ-WP-TM-2013-0142 HAS BEEN REVIEWED AND IS APPROVED FOR PUBLICATION IN ACCORDANCE WITH ASSIGNED DISTRIBUTION STATEMENT.

*//Signature//
TOM A. PRESDORF, Project Engineer
Aero Validation Branch
Aerospace Vehicles Division
Aerospace Systems Directorate

//Signature//
LAWRENCE M. LENY, Chief
Aero Validation Branch
Aerospace Vehicles Division
Aerospace Systems Directorate

This report is published in the interest of scientific and technical information exchange, and its publication does not constitute the Government's approval or disapproval of its ideas or findings.

*Disseminated copies will show "//Signature//" stamped or typed above the signature blocks.

REPORT DOCUMENTATION PAGE

Form Approved
OMB No. 0704-0188

The public reporting burden for this collection of information is estimated to average 1 hour per response, including the time for reviewing instructions, searching existing data sources, gathering and maintaining the data needed, and completing and reviewing the collection of information. Send comments regarding this burden estimate or any other aspect of this collection of information, including suggestions for reducing this burden, to Department of Defense, Washington Headquarters Services, Directorate for Information Operations and Reports (0704-0188), 1215 Jefferson Davis Highway, Suite 1204, Arlington, VA 22202-4302. Respondents should be aware that notwithstanding any other provision of law, no person shall be subject to any penalty for failing to comply with a collection of information if it does not display a currently valid OMB control number. **PLEASE DO NOT RETURN YOUR FORM TO THE ABOVE ADDRESS**.

1. REPORT DATE *(DD-MM-YY)*	2. REPORT TYPE	3. DATES COVERED *(From - To)*
February 2013	Interim	02 July 2012 – 14 February 2013

4. TITLE AND SUBTITLE
COMPUTATIONAL ANALYSIS OF DIFFUSER PERFORMANCE FOR THE SUBSONIC AERODYNAMIC RESEARCH LABORATORY (SARL)

5a. CONTRACT NUMBER
In-house

5b. GRANT NUMBER

5c. PROGRAM ELEMENT NUMBER
62201F

6. AUTHOR(S)
Tom A. Presdorf (AFRL/RQVX)
Christopher D. King, Semih M. Ölçmen, and Muhammad A.R. Sharif (The University of Alabama)

5d. PROJECT NUMBER
N/A

5e. TASK NUMBER
N/A

5f. WORK UNIT NUMBER
Q07S

7. PERFORMING ORGANIZATION NAME(S) AND ADDRESS(ES)
Aero Validation Branch (AFRL/RQVX)
Aerospace Vehicles Division
Air Force Research Laboratory, Aerospace Systems Directorate
Wright-Patterson Air Force Base, OH 45433-7542
Air Force Materiel Command, United States Air Force

The University of Alabama
Aerospace Engineering and Mechanics
205 Hardaway Hall
401 7th Avenue, Box 870280
Tuscaloosa, AL 35487-0280

8. PERFORMING ORGANIZATION REPORT NUMBER

9. SPONSORING/MONITORING AGENCY NAME(S) AND ADDRESS(ES)
Air Force Research Laboratory
Aerospace Systems Directorate
Wright-Patterson Air Force Base, OH 45433-7542
Air Force Materiel Command
United States Air Force

10. SPONSORING/MONITORING AGENCY ACRONYM(S)
AFRL/RQVX

11. SPONSORING/MONITORING AGENCY REPORT NUMBER(S)
AFRL-RQ-WP-TM-2013-0142

12. DISTRIBUTION/AVAILABILITY STATEMENT
Approved for public release; distribution unlimited.

13. SUPPLEMENTARY NOTES
PA Case Number: 88ABW-2013-0955; Clearance Date: 26 Feb 2013. This report contains color.

14. ABSTRACT
Improving the efficiency of the Air Force Subsonic Aerodynamic Research Laboratory (SARL) wind tunnel with the use of alternative diffuser geometries is investigated. A previous analysis of head losses throughout the tunnel has shown that, approximately thirty percent of losses through the tunnel occurred at the exit of the tunnel (Britcher, 2011). In the present work, two separate diffuser geometries, identified after precursory calculations made using SolidWorks, were computationally evaluated using the ANSYS FLUENT CFD code to determine their efficiency improvement with respect to the original tunnel geometry and with respect to each other.

Computations were made on the full scale model of the fan duct and the diffuser sections with an average inlet velocity of sixty meters per second, using both uniform and fully developed velocity profiles at the entrance of the fan duct since the velocity profile in the SARL tunnel is not known. The results indicate that a 3.5° half-apex angle conical diffuser followed with tubular and annular conical section with dividers results in the least total pressure loss. The calculated percent head loss reductions for this diffuser geometry range from 14.9% to 20.9% over the existing SARL diffuser geometry. For the entire SARL tunnel, this corresponds to a substantial 5.2% to 7.3% efficiency improvement.

15. SUBJECT TERMS
SARL Diffuser Efficiency

16. SECURITY CLASSIFICATION OF:			17. LIMITATION OF ABSTRACT:	18. NUMBER OF PAGES	19a. NAME OF RESPONSIBLE PERSON (Monitor)
a. REPORT	b. ABSTRACT	c. THIS PAGE			Robert W. Guyton
Unclassified	Unclassified	Unclassified	SAR	30	19b. TELEPHONE NUMBER *(Include Area Code)* N/A

Table of Contents

Approved for public release; distribution unlimited.

Figures

Tables

Approved for public release; distribution unlimited.

1. INTRODUCTION

The Subsonic Aerodynamic Research Laboratory (SARL) wind tunnel, which is designed to operate up to Mach = 0.6, limited to Mach 0.5, is driven by a 20,000 HP motor, located approximately 30 ft (9.14m) outside the tunnel exit (Wright-Patterson AFB, 1992).The motor drives an approximately 2 to 1 increasing gearbox. The tunnel has a 46 ft by 50 ft (14.02 m by 15.24 m) inlet area, and has a 36:1 contraction ratio at the test section. The tunnel was designed for flow visualization and accurate measurements at low-cost and it allows for a 360° line-of-sight of the model in the test section. Turbulence intensity in the test section is reported as 0.05% or below.

Figure 1 provides a schematic drawing of the SARL wind tunnel, and **Figure 2** provides a drawing of the fan duct and diffuser section being considered in this research. The fan duct was designed to house two-stages of fan blades, stator vanes, anti swirl vanes and a nacelle. The fan was originally used in a NASA Langley tunnel. Only the upstream blade set is installed in the SARL. The nacelle is held in place with biconvex struts that are placed 120° apart from each other oriented in a Y configuration at the entrance section, and in an inverted Y configuration, at the aft section of the diffuser. The average tunnel velocity at the entrance to the fan duct, U, is calculated to be 60 m/s when the test section Mach number is 0.5.

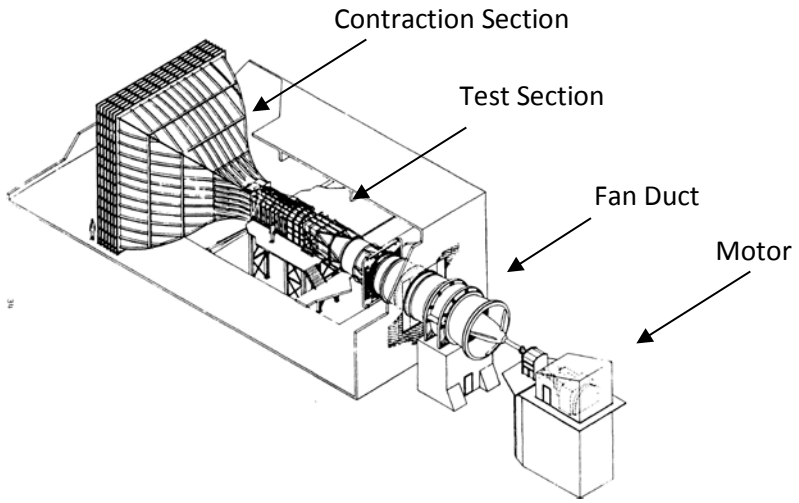

Figure 1 - Schematic drawing with labels of the SARL wind tunnel (Wright-Patterson AFB, 1992)

Approved for public release; distribution unlimited.

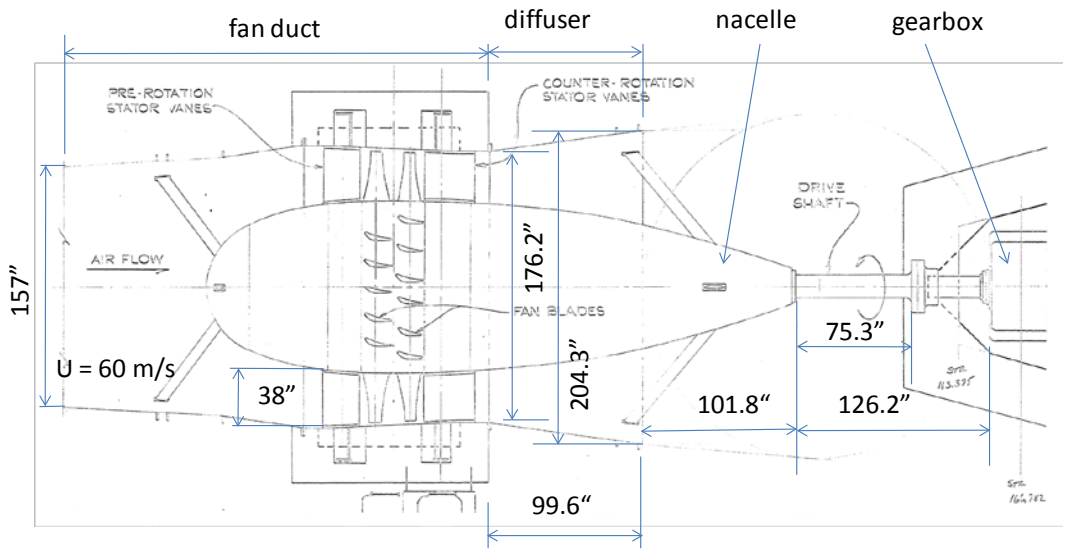

Figure 2 - Drawing of Fan Duct and Exit Diffuser Section of the SARL Wind Tunnel (Wright-Patterson AFB, 1992)

Previous analysis of cumulative losses throughout the tunnel indicated that approximately 30% of all losses in the tunnel occurred at the tunnel exit (Britcher, 2011). In that work, the geometry of the entire tunnel was considered and the losses were expressed using a section total pressure loss coefficient given as:

$$K_0 = \frac{\Delta p_0}{q_{ts}} = K\frac{q_{local}}{q_{ts}} = K\left(\frac{V_{local}}{V_{ts}}\right)^2 \quad (1)$$

where ΔP_0 is the change in total pressure across a given location, q_{ts} is the dynamic pressure at the test section, q_{local} is the dynamic pressure at a specified location, K is the local total pressure loss coefficient, V_{ts} is the velocity magnitude at the test section, and V_{local} is the velocity magnitude at a specified location, respectively. **Figure 3** provides a graphical representation of the results of the study, showing the cumulative total pressure loss coefficient, ($\sum K_0$), versus the position within the tunnel.

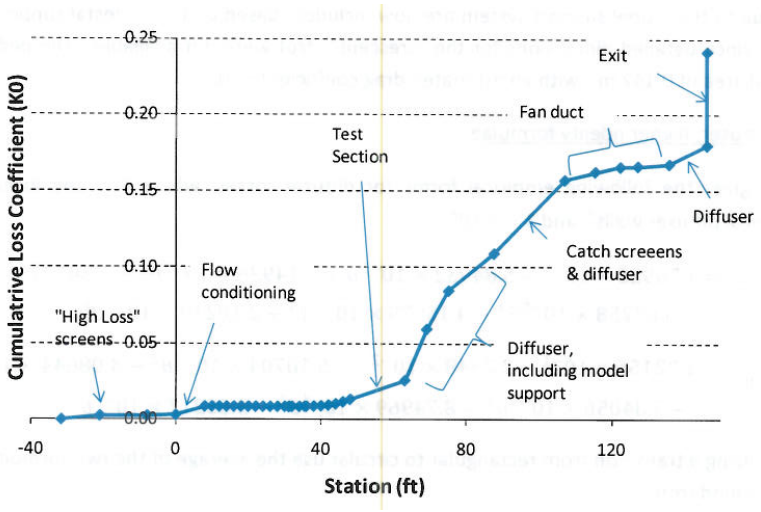

Figure 3 - SARL Cumulative power loss coefficient analysis Britcher, 2011)

Approved for public release; distribution unlimited.

In **Figure 3**, the data points starting at “Fan Duct” and extending to “Exit” represent the portion of the tunnel that is being analyzed in this work. The results of the work by Britcher (2011) showed that the cumulative loss coefficient was about 0.245. The study concluded that the circuit losses were “dominated” by the diffuser and exit sections of the tunnel. If the exit loss coefficient could be reduced, a significant reduction in losses could be observed for the entire tunnel, up to approximately 16% reduction based on analytical study as noted by Britcher, (2011).

The current research was thus focused on minimizing the losses by modifying the diffuser of the wind tunnel. In order to achieve this goal, several diffuser geometries were identified and evaluated for effectiveness in loss reduction. Computational methods were used due to the very large size of the tunnel limiting experimental evaluation of the models. Preliminary computations were made using SolidWorks CAD program. Numerical models of over thirty widely varying diffuser geometries were developed based on previous knowledge on diffuser geometries (Farokhi, 2009; Eckert et al., 1976; Sovran and Klomp, 1967; Mehta, 1977; Townsend, 1976; Lefebvre, 1999; Dixon, 2005) and evaluated for effectiveness in reducing losses for the SARL tunnel. Literature survey showed that, previous systematic research undertaken on conical diffusers was mainly focused on studying empty conical diffusers (Fox an McDonald, 1966; Sovran and Klomp, 1967; Azad, 1996; Lefebvre, 1999; Dixon, 2005). These studies indicate that, (*i*) the ratio of the exit to entrance areas and the length of the diffuser are the parameters directly affecting the pressure recovery performance of the conical diffusers (Lefebvre, 1999), (*ii*) the pressure recovery becomes independent of the Reynolds number over Re = 75000 (Fox and McDonald, 1966, Sparrow et al., 2009), and (*iii*) the diffusers with apex angle ~7° has the best performance (Fox and McDonald, 2010). It appears that research on the annular conical diffusers was focused on investigation of different configurations for specific applications (Johnston, 1953; Ganesan, 1980; Shuja and Habib, 1996; Ubertini and Desideri, 2000; Cherry et al., 2010; Lo et al., 2012).

The models evaluated earlier using the SolidWorks code included conventional and unconventional geometries, such as two diffusers, diffusers redirecting the flow away from the ground, diffusers with splitter plates, conical/annular diffusers of different lengths, combination of conical diffusers, and constant diameter sections with varying lengths. Each diffuser model was created using SolidWorks CAD program and CFD solutions were obtained using the FloWorks add-on flow analysis tool. The FloWorks solves the Favre averaged Navier-Stokes equations using the standard k-ε turbulence model (Launder and Spalding, 1974). **Figure 4** illustrates a few representative examples of the diffuser geometries considered. Due to the close proximity of the gear box housing to the exit of the tunnel, all designs had their lengths restricted to less than 14 ft (4.26 m) since the diffuser was to fit between the tunnel exit and the gear box housing . During the computations, the effects of the blade rotation on the flow field were excluded since it would have required very large computational resources. The blades were also excluded from the geometry to study the effects of only the diffuser geometry on the efficiency calculations.

Approved for public release; distribution unlimited.

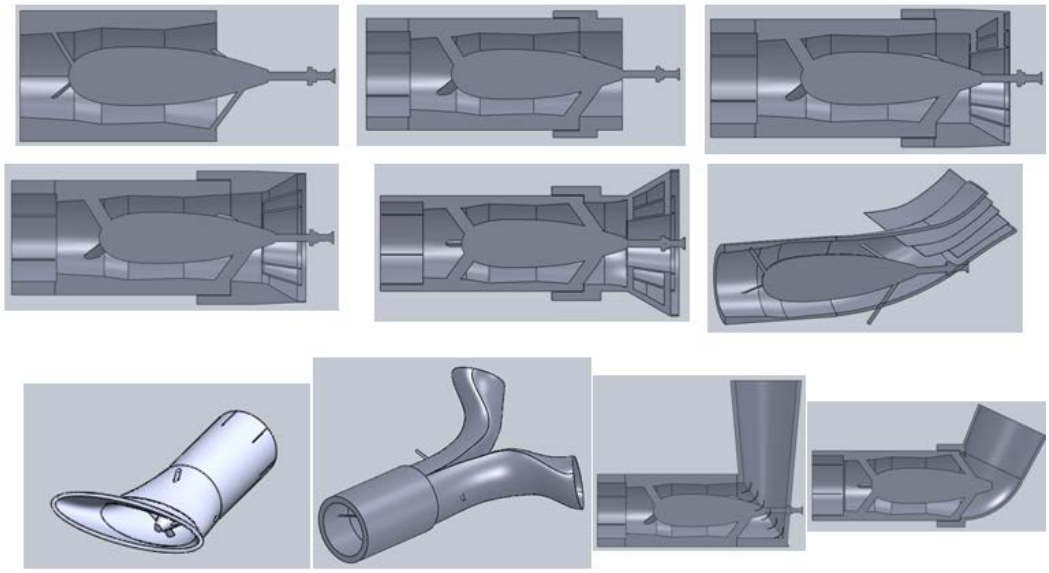

Figure 4 - SARL Example Diffuser Designs Tested using SolidWorks

Out of the 30 different diffuser geometries analyzed by the FloWorks code, 4 specific geometries were selected for analysis by the ANSYS FLUENT code. These include the existing SARL diffuser (baseline model) with a 8° half-apex angle, henceforth termed as "8BT," and a modified version of it with a 3.5° half-apex angle, henceforth termed as "35BT." The 3.5BT was modified simply by adding a constant area diffuser at the end, henceforth termed as "35F" which was further modified with an additional annular conical diffuser after the flat section, henceforth termed as "35FC". The 35FC consisted of 3 concentric truncated cones with included angles of 60°, 34.7°, 17.2°, and the entrance area to the inner cone was equal to the entrance areas between the successive cones. The flat and the conical sections had the same length. The 35F and the 35FC configurations were selected because they produced greatest reduction in pressure losses and about 6% improvement in the entire tunnel efficiency when analyzed with the FloWorks code. These 4 diffuser configurations are shown in **Figure 5**.

Approved for public release; distribution unlimited.

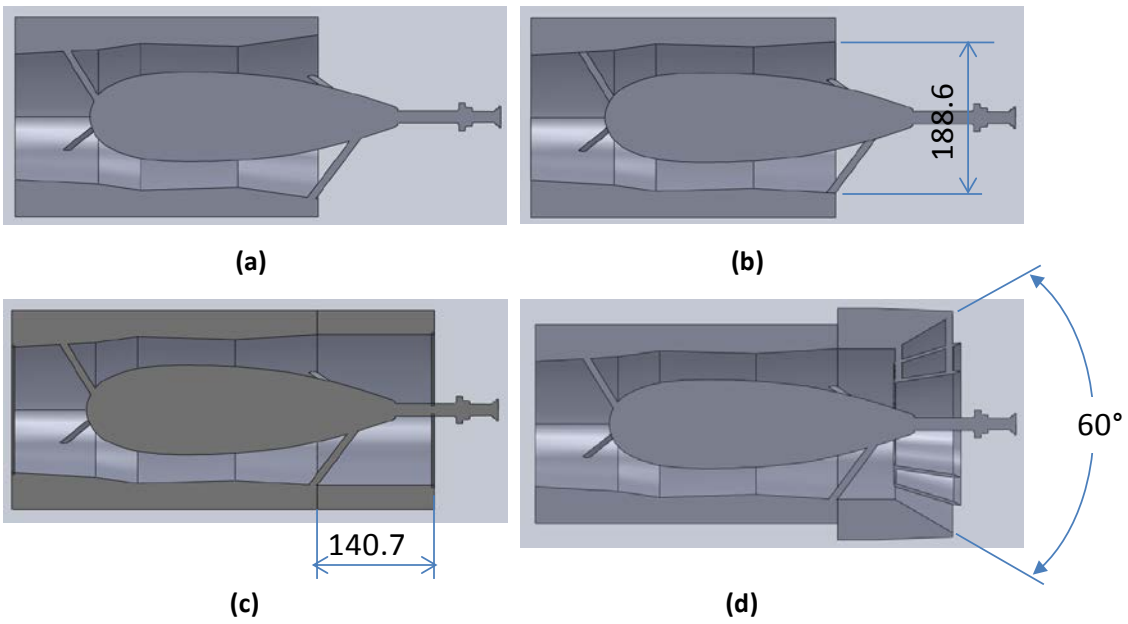

Figure 5 - Sectional views of the 4 diffuser configurations; a) 8BT, b) 35BT, c) 35F, d) 35FC

For each of these models, both uniform and fully developed inlet flow conditions were used. Computations were made on full scale models of the existing SARL tunnel. Thus computations were performed for a total of 8 different configurations. **Table 1** presents the summary matrix of the various computations performed in this study. The Reynolds number for these computations is based on the average inlet velocity and the duct diameter at the inlet section for air at 15°C. The Reynolds number for the full scale models were taken as 1.647×10^{7}.

Table 1 - Full Matrix of Computations by Model and Boundary Conditions

	3D Full Size ($Re = 1.647\times10^{7}$)
Grid independence study	8BT, 35FC
Uniform inlet flow	8BT, 35BT, 35F, 35FC
Fully developed inlet flow	8BT, 35BT, 35F, 35FC

Approved for public release; distribution unlimited.

2. NUMERICAL PROCEDURE AND PROBLEM SETUP

The Reynolds-Averaged Navier-Stokes (RANS) equations were solved using the ANSYS FLUENT commercial code with the standard k-ε turbulence model (Launder and Spalding, 1974). The governing equations and turbulence model constants are available in FLUENT user manual and are not repeated here. The flow domain is divided into many small finite volumes with an unstructured mesh. A collocated arrangement for the placement of the flow variables is used in the mesh system. The conservation equations are integrated over each of the finite volume to yield sets of linear algebraic equations. These sets of linear algebraic equations are then solved sequentially using an iterative method. The SIMPLE (Patankar, 1980) algorithm is used for the pressure-velocity coupling. The convective fluxes have been calculated using the second order upwind scheme while the diffusive fluxes have been calculated using the central difference scheme. The convergence is assumed when the value of the scaled residual of continuity and momentum equations is less than 10^{-6}. Convergence has also been monitored by plotting the drag on the nacelle surface until the variation of the drag leveled off with iteration.

2.1 Geometry and Mesh Design.

The flow configuration geometry was created using the SolidWorks code which was imported into ANSYS FLUENT for mesh generation. The computational mesh was generated using the meshing code integrated in the ANSYS package. The solid bodies, such as the outer diffuser, fan duct wall, engine nacelle, and support spars had a “face sizing” mesh control applied to these surfaces, with a slow smoothing method applied to the domain from these locations. This created an unstructured grid that had the highest mesh refinement near the actual diffuser geometry, which slowly became coarser farther away from these surfaces. The flow domain consists of two parts; the base tunnel fan-duct and diffuser from the inlet to the exit (the region between the outer casing and nacelle surface, the downstream diffuser section, and the upstream inlet duct section) and, the downstream open rectangular wake region as shown in **Figure 6**. A close up view of the sample base configuration surface mesh is shown in **Figure 7**.

Approved for public release; distribution unlimited.

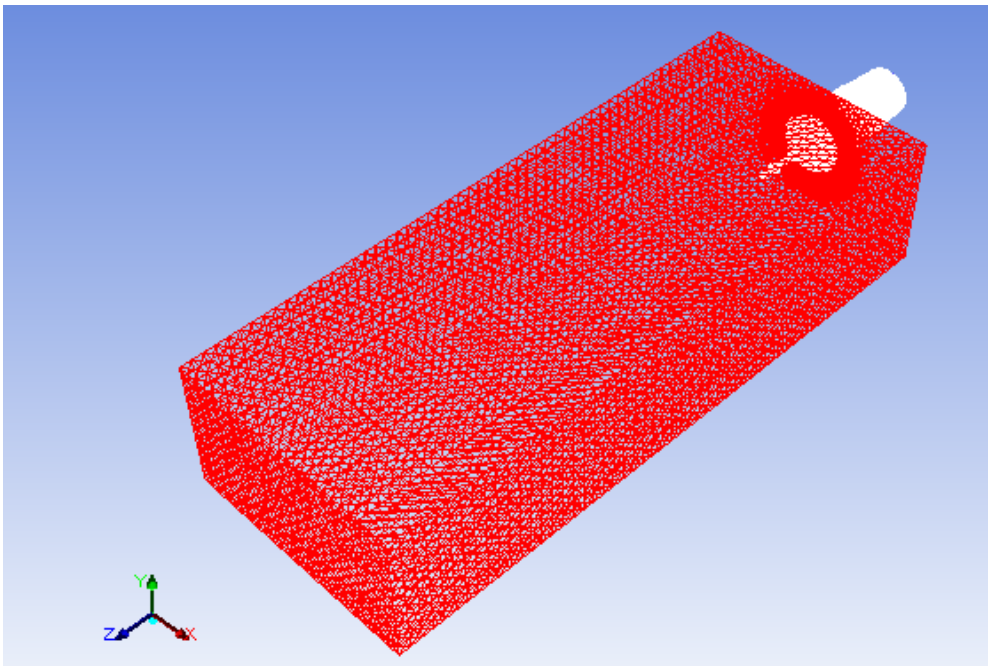

Figure 6 - Sample Mesh of Base Diffuser Geometry for Entire Computational Domain for 8 Base Configuration in ANSYS FLUENT.

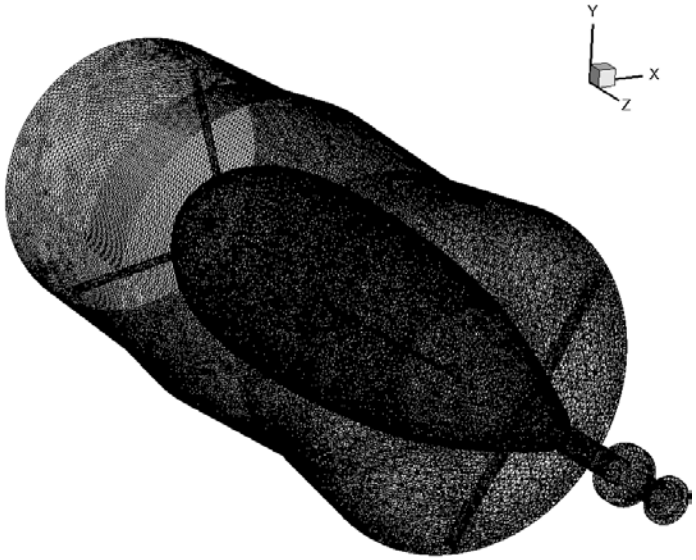

Figure 7 - Sample Mesh of Base Diffuser Geometry showing Surface Meshing for 8 Base Configuration in ANSYS FLUENT.

The three-dimensional domain required a large number of cells (of the order of a few million) to fill.

Approved for public release; distribution unlimited.

2.2 Boundary Conditions

For all computations the no-slip condition was imposed on all solid walls or surfaces including the nacelle surface, tunnel casing wall, on the strut rod surfaces, etc. Constant pressure outlet condition was imposed on all open boundaries of the downstream rectangular wake region where the values of the velocity components are extrapolated from inside. As mentioned earlier, two types of inlet conditions were used in the computations; (*i*) uniform axial velocity compatible to the corresponding Reynolds number with other velocity components being zero and (*ii*) a fully developed mean axial velocity component with average velocity compatible to the Reynolds number. The uniform inlet velocity condition is straight forward to implement. For the fully developed inlet velocity condition, the profile was obtained through separate turbulent flow simulation in a circular pipe of length greater than the entry length, which is given by $4.4(D)(\mathrm{Re}^{1/6})$, where D is the pipe diameter and Re is the Reynolds number (given in Table 1) based on the average velocity. A uniform velocity of 60m/s was input as the velocity entering the pipe and the profile at the exit of this pipe was specified as the tunnel section inlet velocity condition through the user defined function feature of the FLUENT code.

2.3 Grid Independence Study

In order to obtain mesh independent results, systematic mesh independence study was conducted. Starting with a basic coarse mesh with few hundred thousand cells, the mesh was successively refined and the computed shear stress distributions along the nacelle top surface as well as the total pressure profiles at the diffuser exit along the y-mid-pane were compared. The mesh was considered optimally refined when the plots of the shear stress and total pressure distribution did not change appreciably between successive mesh refinements.

Figures 8 and 9 provide examples of the results of grid independence studies for the corresponding geometry mentioned in the plot title. Once grid independence was established for the original diffuser geometry, the same mesh settings were applied to the other geometries, as the changes were assumed relatively minor. One exception to this was the diffuser geometry that made use of conical sections to split the flow at the exit of the diffuser (35FC case). A separate grid independence study was made for this geometry.

Approved for public release; distribution unlimited.

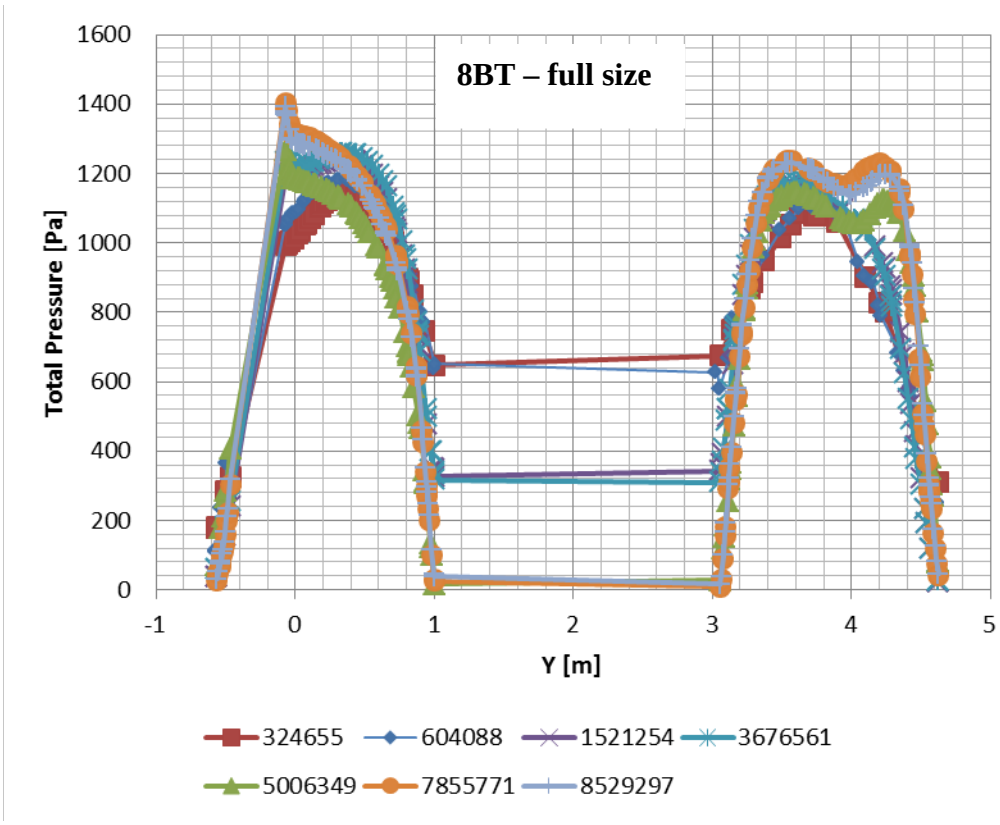

Figure 8 - Variation of total pressure at the diffuser section exit plane, along the central line in the y-direction, with mesh refinement. Numbers at the bottom represent total number of cells for each mesh.

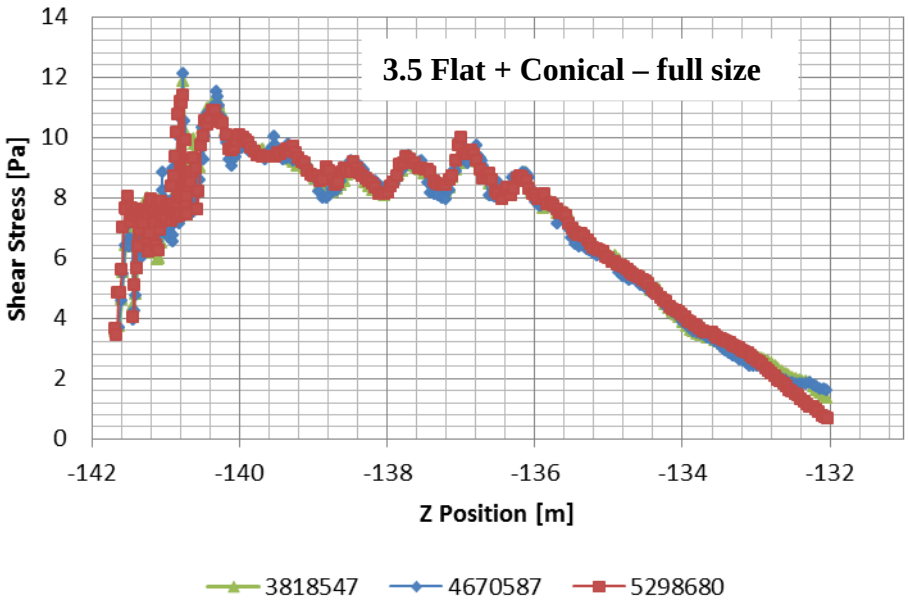

Figure 9 - Variation of shear stress along engine nacelle top surface with mesh refinement. Numbers at the bottom represent total number of cells for each mesh

Approved for public release; distribution unlimited.

3. RESULTS AND DISCUSSION

For the SARL tunnel, the head loss is considered in two parts: the head loss within the fan duct and diffuser, and the head loss of the flow exiting the diffuser. **Figure 10** represents the locations for which these losses are associated. Here location 1 and 2 represent the entrance and exit sections of the diffuser while location 3 represents a section outside the exit of the diffuser which is sufficiently far away so that the velocity at this location is essentially zero. The total head loss for sections 1-2 and 2-3, can be expressed with the following equations:

$$h_{L_{1-2}} = \frac{(P_1 - P_2) + \frac{1}{2}\rho(V_1^2 - V_2^2)}{\rho g} \tag{2}$$

$$h_{L_{2-3}} = \frac{\frac{1}{2}V_2^2}{g} \tag{3}$$

$$h_{L_{total}} = h_{L_{1-2}} + h_{L_{2-3}} \tag{4}$$

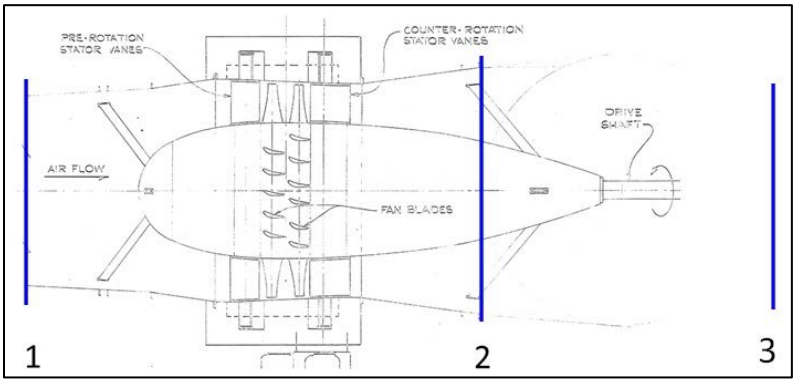

Figure 10 - General locations for power loss calculations relative to the SARL wind tunnel fan duct and diffuser sections.

Since the head losses are directly related to the change in the total pressure from the inlet to the exit of the diffuser, the total pressure distributions both in the fan duct and the diffuser sections are investigated. The total pressure distribution for the original configuration, 8BT, with uniform inlet velocity condition is shown in **Figure 11**. The flooded contours of the total pressure distribution, at the diffuser exit section and on a longitudinal plane in the axial direction, are shown on the left and right, respectively, in this figure. The longitudinal flow direction in this and other subsequent figures is from left to right. Additional contours of velocity magnitude distribution through the geometry for the same case are provided in **Figure 12** to visualize potential locations of flow separation and diffusion**.**

Approved for public release; distribution unlimited.

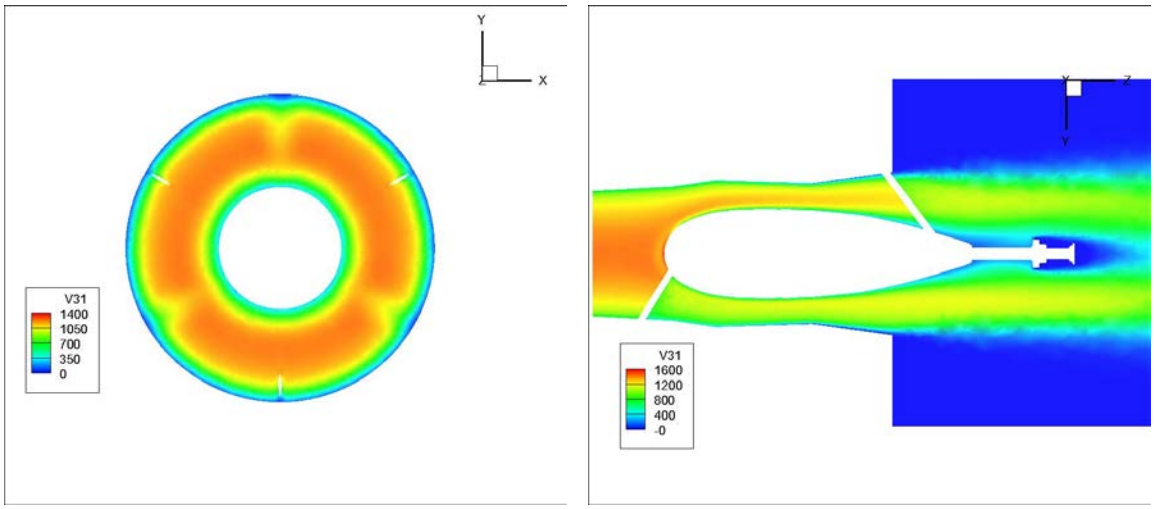

Figure 11 - Total pressure distribution through 8BT - uniform inlet flow.

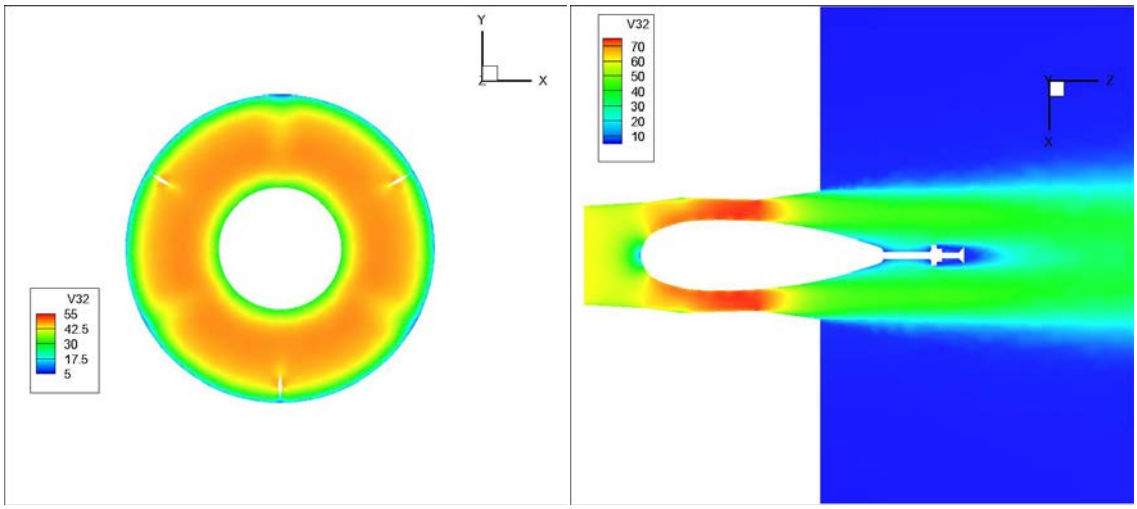

Figure 12 -Velocity magnitude distribution through 8BT - uniform inlet flow.

It can be seen that the flow does begin to slow significantly along the 8° angle diffuser section, and the velocity distribution at the exit is generally uniform and axisymmetric. To compare this to the fully developed flow condition at the inlet, the distribution of the velocity through the model has been provided in **Figure 13**.

Approved for public release; distribution unlimited.

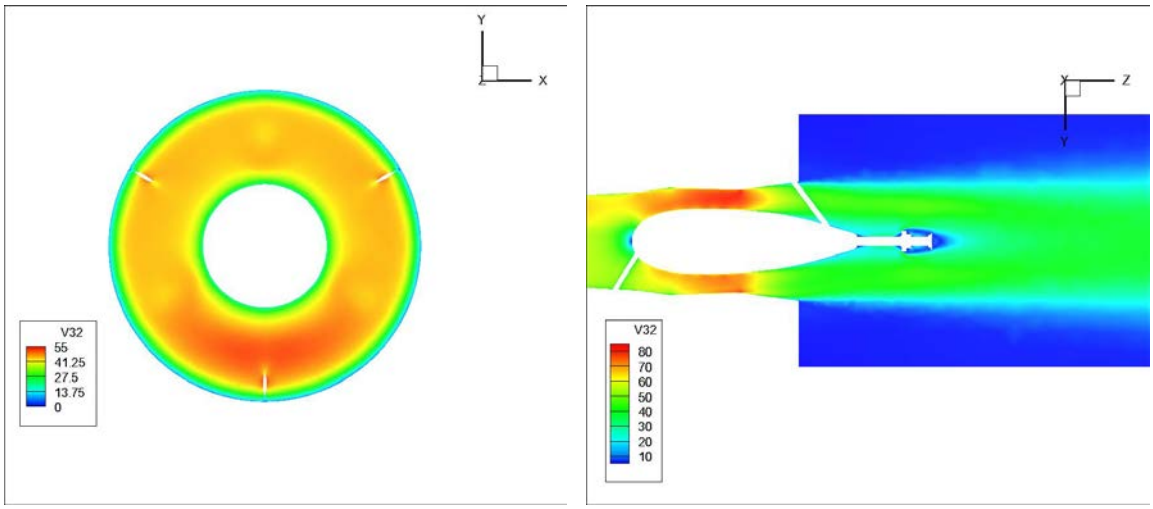

Figure 13 - Velocity magnitude distribution through 8BT - fully developed inlet flow.

While the velocity distribution within the fan duct and diffuser does differ slightly from that of the uniform flow case, the velocity distribution at the exit does have one region of notable difference from the uniform inlet flow case. The velocity distribution at the exit of the 8BT for a fully developed inlet flow is generally uniform, but shows a region of increased velocity along the bottom of the exit between 120° and 240° counterclockwise from the top of the exit section. This altered velocity distribution could be attributed to the flow remaining attached a greater distance for fully developed flow than for uniform flow within the diffuser, and to the interference of a support spar directly immediately upstream of the exit.

Next, the 35BT geometry is considered. **Figure 14** represents the total pressure distribution through the model for the uniform inlet flow case, while the **Figure 15** represents the velocity magnitude distribution through the geometry.

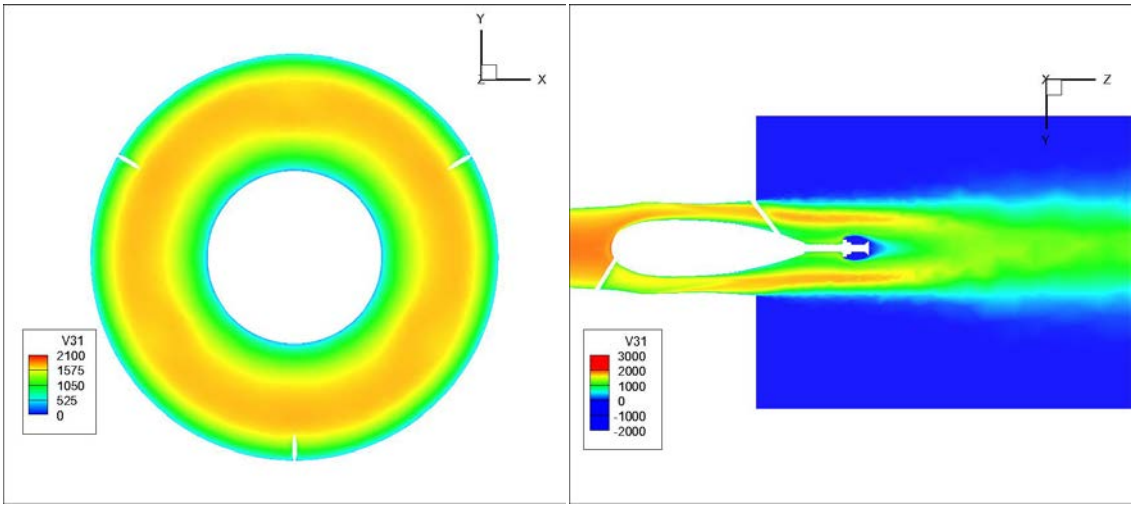

Figure 14 - Total pressure distribution through 35BT - uniform inlet flow.

Approved for public release; distribution unlimited.

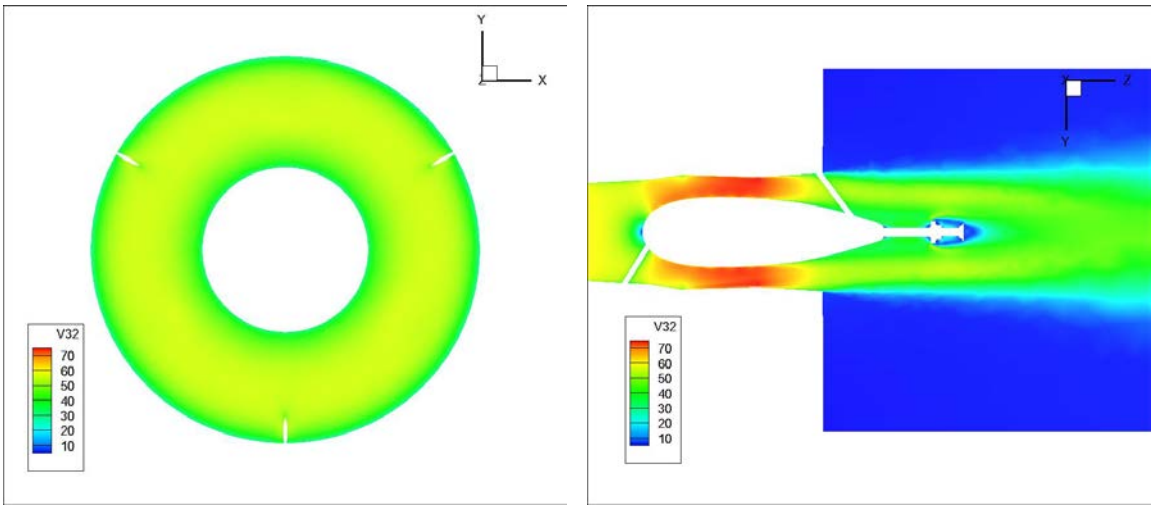

Figure 15 - Velocity magnitude distribution through 35BT - uniform inlet flow.

Compared to the distributions of total pressure and velocity magnitude observed in the 8BT model, it seems that there is a greater degree of diffusion occurring in the flow near the exit of the 35BT diffuser that is likely to lead to greater losses. To visualize and compare the differences between the uniform inlet flow and fully developed flow cases, the velocity distribution through the full size 35BT geometry for fully developed inlet flow is shown in **Figure 16**.

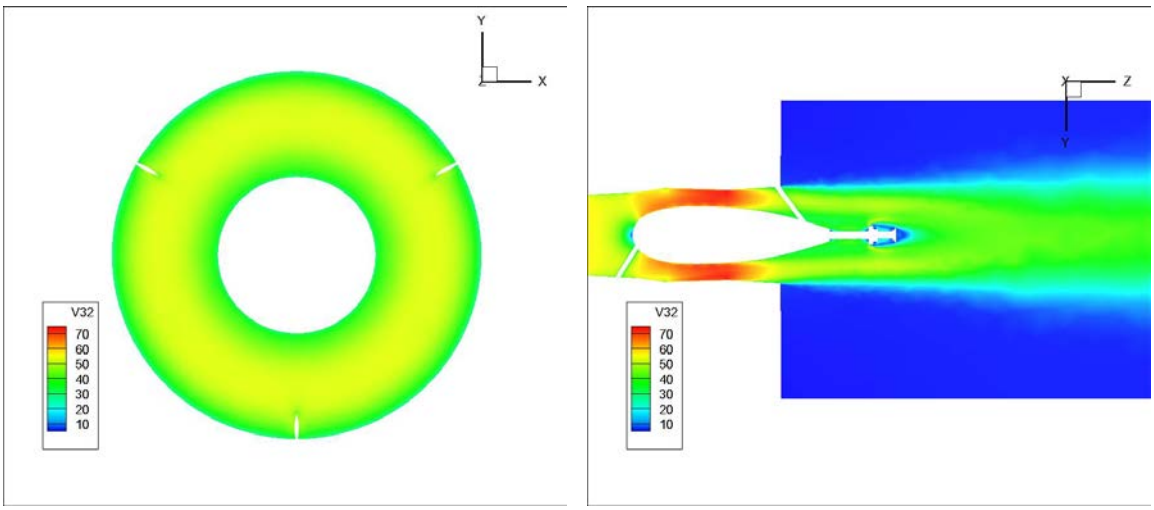

Figure 16 - Velocity magnitude distribution through 35BT - fully developed inlet flow.

For both the uniform and fully developed flow cases, the flow travelling through the 35BT geometry encounters the same diffusion as it nears the exit of the diffuser.

A similar comparison of the total pressure and velocity magnitude distributions of the 35F, and 35FC models is presented for comparison to the baseline geometry. **Figure 17** represents the total pressure distributions, while **Figure 18** represents the velocity magnitude distributions through the full size 35F diffuser model under uniform inlet flow conditions.

Approved for public release; distribution unlimited.

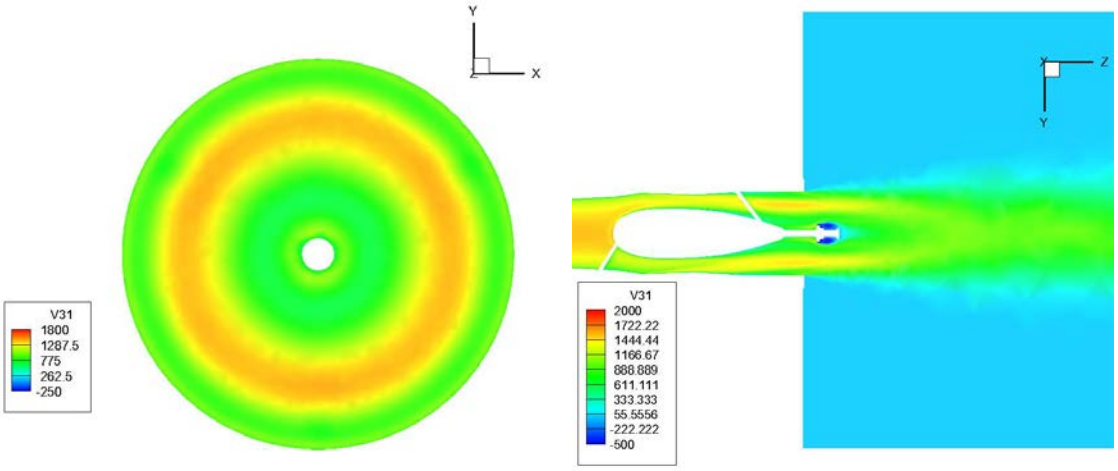

Figure 17 - Total pressure distribution through 35F - uniform inlet flow.

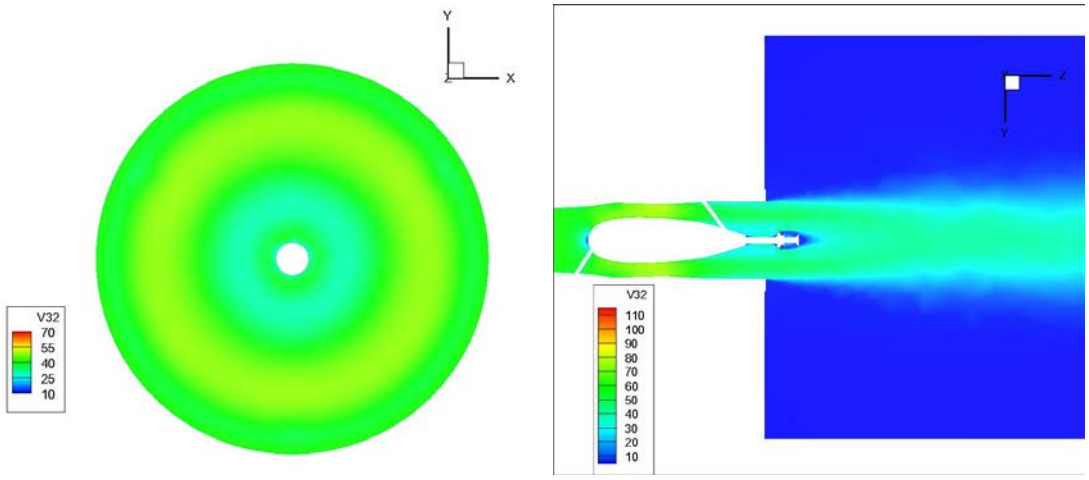

Figure 18 - Velocity magnitude distribution through 35F - uniform inlet flow.

The figures indicate that the velocity of the flow exiting the 35F full size model is lower than that of the baseline geometry (35BT). In addition, the flow can be observed to slow following the surface of the engine nacelle near the exit of the diffuser, compared to that of the 35BT.

The **Figure 19** shows the velocity distribution through the 35F under fully-developed inlet conditions. Velocity distribution is similar to the distribution obtained with the uniform inlet flow case. The flow velocity peaks in a doughnut section closer to the mid section of the duct, the flow near the nacelle has decreased velocity values.

Approved for public release; distribution unlimited.

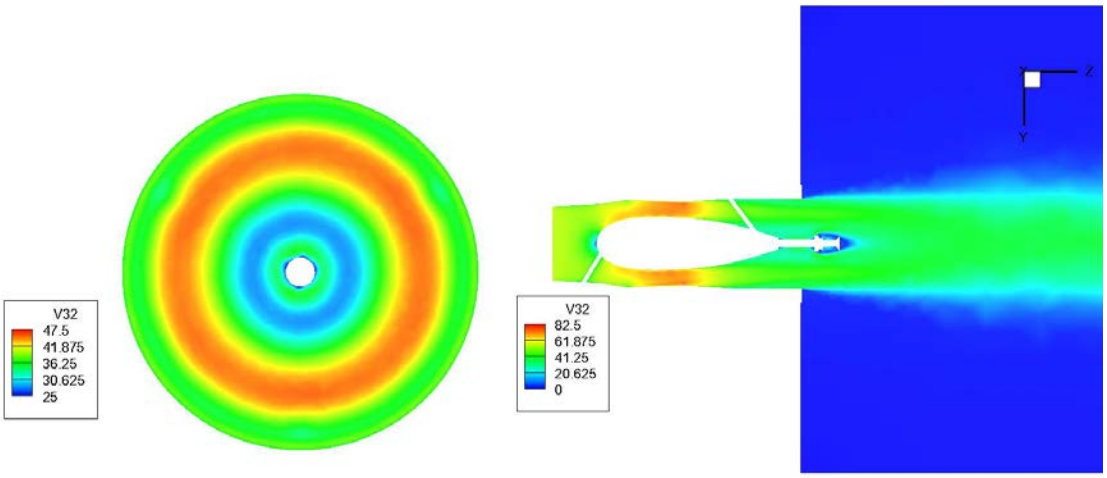

Figure 19 - Velocity magnitude distribution through 35F - fully developed inlet flow

Figures 20 and 21 represent the total pressure and velocity distributions, respectively, of the full size 35FC diffuser geometry.

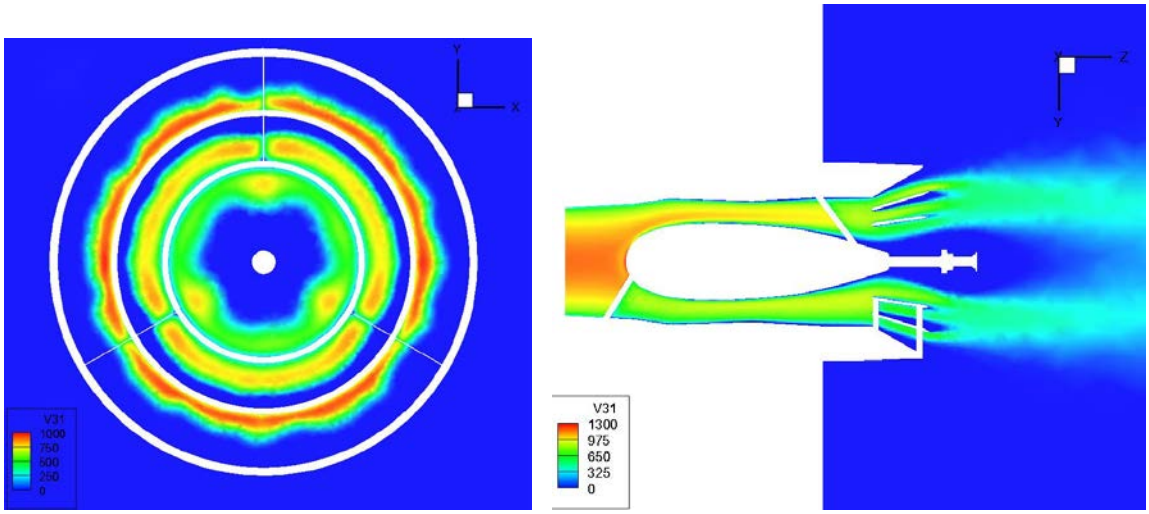

Figure 20 - Total pressure distribution through 35FC - uniform inlet flow.

Approved for public release; distribution unlimited.

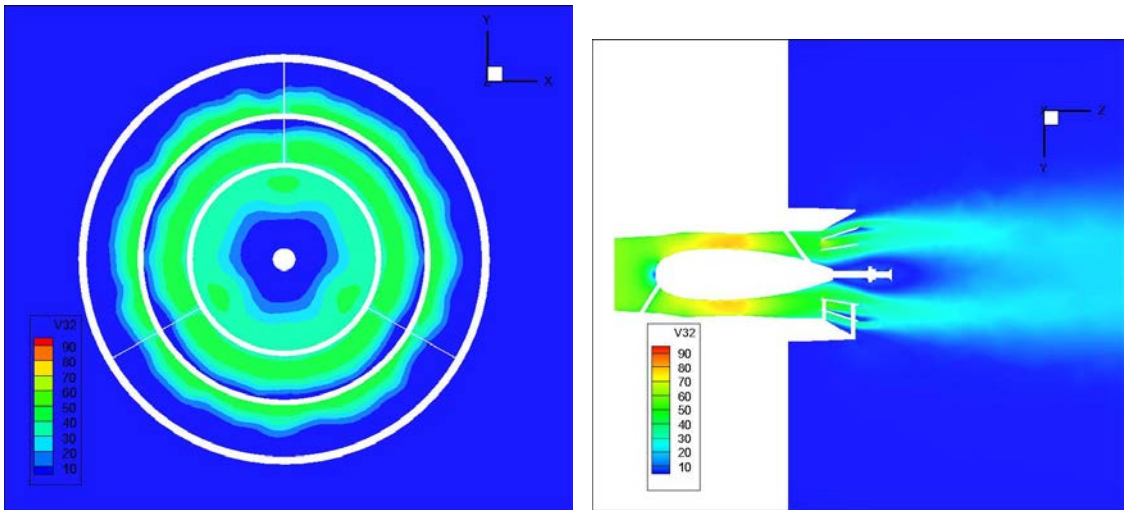

Figure 21 - Velocity magnitude distribution through 35FC - uniform inlet flow.

Figures indicate that the total pressure exiting the diffuser is essentially at atmospheric conditions and that the flow through the fan duct section is free of separation. However, within the conical region of the diffuser, flow separation occurs along the surface of the cone splitting the flow. The conical sections that are radially further from the center of the diffuser (between the outer and middle cones) have more separation then the middle sections (inner cone and between the inner and middle cones). In addition, the flow that is radially closest to the center of the diffuser is turned by the inner conical section, increasing the spreading rate of the jet exiting the tunnel. Considering the total pressure distribution at the exit of this diffuser geometry, it is expected that the 35FC model will offer the greatest improvement in the reduction of losses.

The flow velocity magnitude obtained with fully developed inlet flow conditions is shown in **Figure 22.** Figure shows that the velocity distribution is very similar to the one obtained with uniform inlet flow conditions but the velocity magnitude is observed to be smaller throughout the fan-duct, diffuser and at the exit.

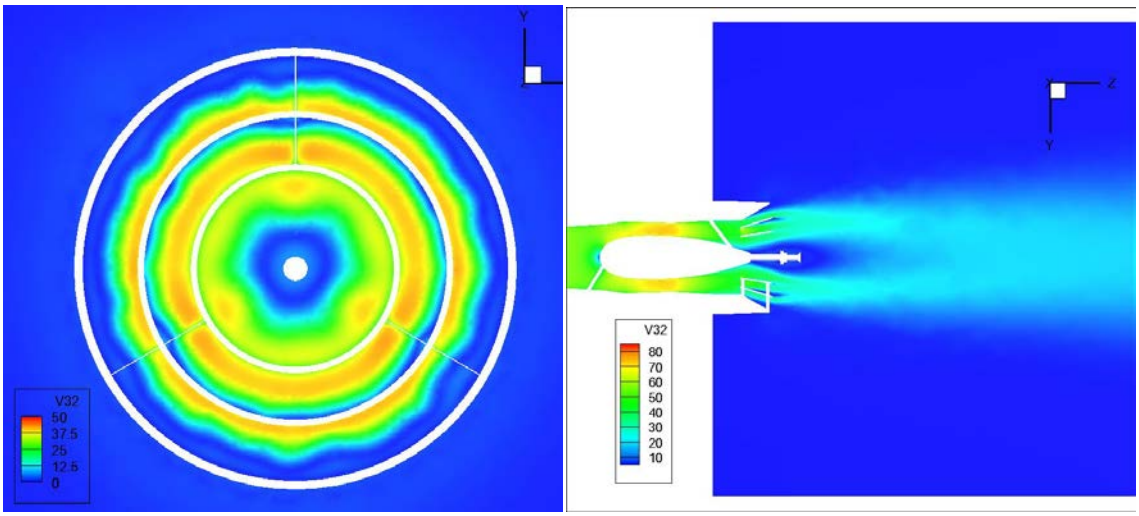

Figure 22 - Velocity magnitude distribution through 35FC – fully developed inlet flow.

Approved for public release; distribution unlimited.

The total head losses associated with the various diffuser configurations are computed using Equations (2) – (4) and are presented in **Table 2** for each model considered in this study.

Table 2 - Calculated head losses (m) at standard pressure and temperature for various diffuser geometries.

Diffuser Configuration	Uniform Inlet Flow	Fully Developed Inlet Flow
8BT	113.04	106.30
35BT	153.80	136.12
35F	108.30	94.54
35FC	96.24	84.12

Results indicate that a fully developed inlet flow leads to a reduction for all the diffuser models, and that the 35FC is the best working model.

A comparison of the percentage improvement of each model relative to the base line (8BT) configuration is compiled into **Table 3**.

Table 3 - Percentage improvement in head losses compared to the base line (8BT) configuration.

Diffuser Configuration	Uniform Inlet Flow	Fully Developed Inlet Flow
35BT	-36.05	-28.05
35F	4.20	11.07
35FC	14.87	20.86

It can be seen that for the full size models, the 35FC diffuser geometry offers the greatest improvement to reducing losses with a range between 14.87% for the uniform inlet flow case to 20.86% for the fully developed flow case. Considering the entire tunnel, this translates to approximately a 5.2% to 7.3% improvement. The 35F geometry also offers an improvement range of 4.20% to 11.07%, which translates to 1.47% to 3.87% range for the entire tunnel. Thus, from the numerical analysis presented here it is concluded that the 35FC diffuser geometry yields maximum pressure recovery in the full size tunnel.

3.1 Further Discussion

As discussed by Lefebvre (1999) based on the research conducted by Sovran and Klomp (1967) the aspect ratio, $AR = A_2/A_1$, and the dimensionless diffuser length, $DL = L/R_1$ of the conical or annular conical diffusers define the pressure recovery of the diffuser rather than the geometry of the annular sections. In these equations, A_1, and A_2 are the entrance and the exit areas of the diffuser, L is the length of the diffuser and, the $R_1 = \sqrt{A_1/\pi}$ is the radius of the diffuser at the entrance. The performance curves generated by Sovran and Klomp (1967) are shown in **Figure 23.** The parameters pertaining to the current diffuser geometries were calculated and are presented in **Table 4**. Parameters were calculated using two separate arguments, in the first case calculations were done as if the diffuser section could be assumed as an empty conical section and thus the nacelle was neglected, in the second case cross sections that were blocked by the nacelle were omitted. Also, in the second case the entrance radius was

Approved for public release; distribution unlimited.

calculated as the radius of a circle that has an area equal to that of the unblocked area. The coordinates of the geometries are shown in **Figure 23**.

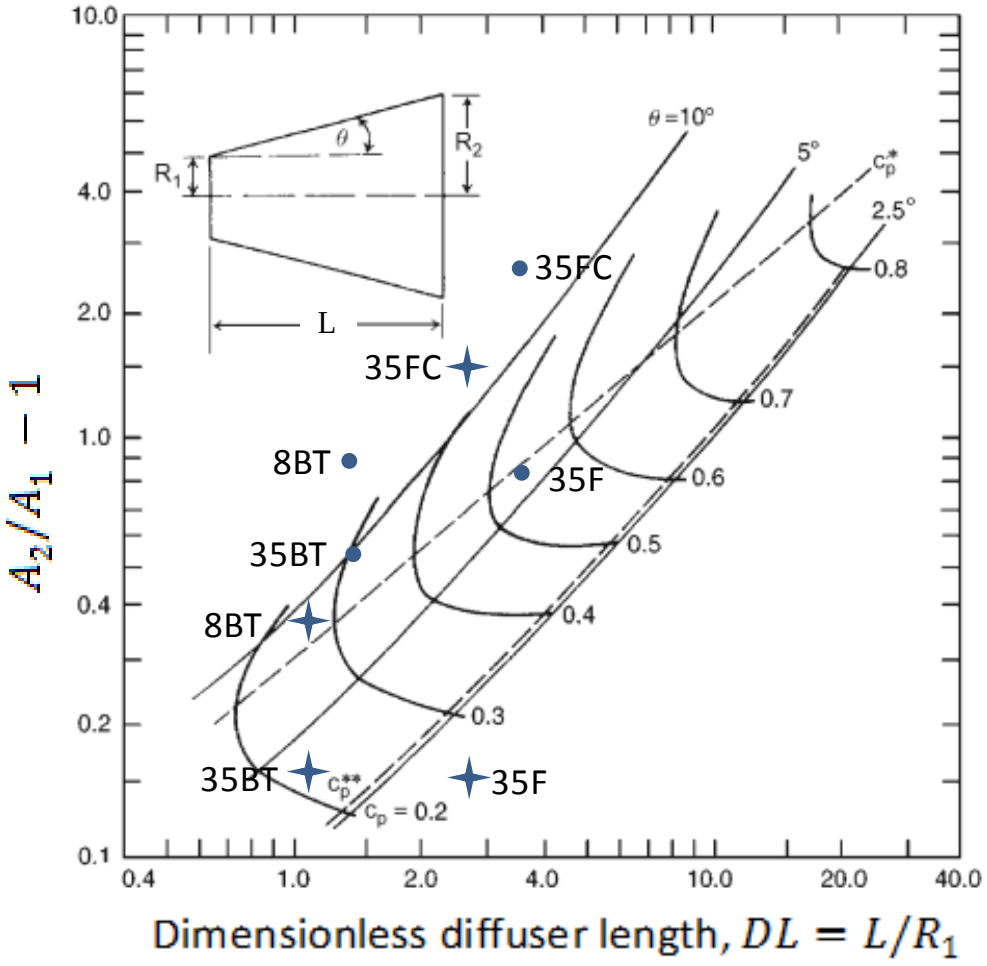

Figure 23 - Performance chart for conical diffusers. (adapted from Sovran and Klomp, 1967).

The Cp* line in **Figure 23** is the locus of points which define the diffuser area ratio producing maximum pressure recovery in a prescribed non-dimensional diffuser length. The Cp** line is the locus of points which define the diffuser non-dimensional length producing maximum pressure recovery at a prescribed area ratio. Cp is the pressure recovery coefficient based on the bulk inlet velocity. The symbols ✦ and ● denotes the empty conical and annular conical cases, respectively.

Approved for public release; distribution unlimited.

Table 4- Calculated head losses (m) at standard pressure and temperature for various diffuser geometries.

geometry	empty conical		annular conical	
	AR	DL	AR	DL
8BT	1.34	1.13	1.83	1.43
35BT	1.15	1.13	1.51	1.43
35F	1.15	2.81	1.83	3.56
35FC	2.39	2.81	3.54	3.57

The parameters were computed in two different ways since it was observed that the 8BT parameters indicated to a point very close to the best pressure recovery line once empty conical argument is made, however the parameters indicate to a point above the $\theta = 10°$ curve for the annular conical argument indicating to a possibility that a different diffuser could be used to improve the performance of the SARL. The correct use of the chart requires using only the areas that allow fluid flow. The 35BT parameters indicate that the annular conical calculations result in a point near the best pressure recovery line, although CFD results showed that this geometry performed poorly. The parameters calculated for the 35F differ drastically from each other. The annular conical argument indicates to the fact that this diffuser is the most likely candidate since the geometry of the diffuser is easy to manufacture and it is the second best performing geometry. The 35FC diffuser geometry that resulted in best performance in CFD calculations resides away from the best performance curve shown by Sovran and Klomp (1967). A similar geometry was discussed by Cheng (1992) as a means to increase the pressure recovery while reducing the diffuser length. Cheng had argued that different conical sections should have a common apex point, and that the flow can be considered as spherically diffusing. The 35FC geometry differs than the one discussed by Cheng (1967) since the conical annular sections are same length. It is believed that the conical sections distribute and force the flow velocity to slow down although they also cause separation in the conical sections. For the application studied in the current paper, the separation closer to the exit is not important since there are no tunnel sections beyond this point. However, separation may cause increased noise levels, which will be studied in a future study.

Approved for public release; distribution unlimited.

4. CONCLUSIONS

The primary goal of this research was to identify the diffuser geometry that would results in greatest reduction in pressure losses for the Subsonic Aerodynamic Research Laboratory (SARL) wind tunnel at the Air Force Research Laboratory. Computational results of two diffuser geometries were compared to each other and to the existing diffuser in providing the maximum pressure recovery. Flow field solutions were obtained at 60 m/s average inlet velocity for both uniform inlet turbulent flow and fully developed inlet turbulent flow.

Results indicate that the 35FC diffuser geometry offered the greatest reduction in pressure losses, yielding 14.87% to 20.86% improvement over the existing SARL tunnel diffuser for the full scale model. Considering the improvement for the entire SARL tunnel, this range is 5.20% to 7.30%. The 35F geometry also offered improvement in the reduction of losses, resulting in 4.20% to 11.07% improvement over the existing SARL diffuser. For the entire SARL tunnel, this range is approximately 1.47% to 3.77% improvement in pressure recovery.

Approved for public release; distribution unlimited.

5. REFERENCES

--, “Subsonic Aerodynamic Research Laboratory”, Wright-Patterson Air Force Base, WL-TR-3053, Wright-Patterson AFB, Cleveland, OH, 1992.

--, “COSMOS 2008: COSMOSFloWorks Fundamentals”, Penn State Personal Web Server: Jeremy Alan Hall [online], URL: http://www.personal.psu.edu/jah5420/Misc/SolidWorks/COSMOSFloWorks/FloWorks/lang/english/Docs/Fundamentals.pdf, Accessed 5/21/12.

--, “ANSYS 12.0: ANSYS FLUENT Theory Guide”, SharcNet [online], URL: https://www.sharcnet.ca/Software/Fluent12/html/th/node3.htm

--, “Entrance Length and Developed Flow”, Engineering Toolbox [online], URL: http://www.engineeringtoolbox.com/entrance-length-flow-d_615.html, Accessed: 3/22/12.

Azad, R.S., 1996, “Turbulent Flow in a Conical Diffuser: A Review”, 1996, *Experimental Thermal and Fluid Science*, Vol. 13, pp. 318-337.

Britcher, Colin P., 2011, “Analysis of the AFRL SARL facility drive system”, Old Dominion University, Department of Mechanical and Aerospace Engineering, Norfolk, VA.

Cheng, Dah Y., 1992, “Large Angle Diffuser Diverter Design for Maximum Pressure Recovery”, US Patent 5,165,452.

Cherry, E.M., Padilla, A.M., Elkins, C.J., and, Eaton, J.K, 2010, “Three-dimensional velocity measurements in annular diffuser segments including the effects of upstream strut wakes”, *International Journal of Heat and Fluid Flow*, Vol. 31, pp.569–575.

Dixon, S.L., 2005, *Fluid Mechanics and Thermodynamics of Turbomachinery*, 2005, fifth edition, Elsevier Publishing Company, ISBN: 0-7506-7870-4

Eckert, W.T., Mort, K.W., Jope, J., 1976, “Aerodynamic Design Guidelines and Computer Program for Estimation of Subsonic Wind Tunnel Performance”, Ames Research Center and U.S. Army Air Mobility R&D Laboratory, NASA TN D-8243, Moffett Field, CA.

Farokhi, S., 2009, *Aircraft Propulsion*, pp. 227-235, John Wiley & Sons, Hoboken, NJ.

Fox, R.W., McDonald, A.T., Pritchard, P.J., 2010, *Fox and McDonald's Introduction to Fluid Mechanics*, Edition 8, ISBN: 0470547553, John Wiley & Sons Incorporated.

Ganesan, V., “ Flow and Boundary Layer Development in Straight Core Annular Diffusers”, 1980, *Int. J. Engng Sci.*, Vol 18, pp. 287-304.

Johnston, I.H., 1953, “The Effect of Inlet Conditions on the Flow in Annular Diffusers”, Memorandum No. M.16, National Gas Turbine Establishment, Pyestock, Hants. Whetstone, Leics.

Launder, B.E., Spalding, D.B., 1974, “The Numerical Computation of Turbulent Flows”, *Computer Methods in Applied Mechanics and Engineering*, Vol. 3, Issue 2, pp. 269-289.

Lefebvre, A. H., 1999, *Gas Turbine Combustion 2nd Edition.*, pp. 77-78., Taylor & Francis, Philadelphia, PA.

Lo. K.P., Elkins, C.J., and Eaton, J.K., 2012, “ Separation control in a conical diffuser with an annular inlet: center body wake separation”, *Exp Fluids*, Vol. 53, pp. 1317–1326.

McDonald, A.T., and Fox, R.W., 1966, “ An Experimental Investigation of Incompressible Flow in Conical Diffusers”, *Int. J. Mech. Sci.*, Vol. 8, pp. 125-139, Pergamon Press Ltd.

Mehta, R.D., 1977, “The Aerodynamic Design of Blow Tunnels with Wide-Angle Diffusers”, *Progress in Aerospace Sciences*, Vol.18, pp. 59-120.

Approved for public release; distribution unlimited.

Patankar, S.V., 1980, *Numerical Heat Transfer and Fluid Flow*," Hemisphere Publishing Corporation.

Schmidt, J., (May 19, 1989 data appended to:) Analysis of the Langley Eight-Foot Transonic Wind Tunnel Fan to be Used as the Drive Fan in the SARL Wind Tunnel, 1986.

Shuja, S.Z., and Habib, M.A., " Fluid Flow and Heat Transfer Characteristics in Axisymmetric Annular Diffusers", *Computers and Fluids***,** Vol. 25, No. 2, pp. 133-150.

Sovran, G., Klomp, E.D., 1967, "Experimentally determined optimum geometries for rectilinear diffusers with rectangular, conical or annular cross-section", In: Sovran, Gino (Ed.), *Fluid Mechanics of Internal Flow*, pp. 272–319. Elsevier Publishing Company.

Townsend, A.A., 1976, *The Structure of Turbulent Shear Flow*, p. 176, Cambridge University Press, Cambridge, MA.

Ubertini, S., and Desideri, U., 2000, "Experimental performance analysis of an annular diffuser with and without struts", *Experimental Thermal and Fluid Science*, Vol. 22 , pp.183 - 195.

Approved for public release; distribution unlimited.